



This is a repository copy of *Minimal impact of late-season melt events on Greenland Ice Sheet annual motion*.

White Rose Research Online URL for this paper:

<https://eprints.whiterose.ac.uk/209382/>

Version: Published Version

Article:

Ing, R.N. orcid.org/0000-0001-9767-3209, Nienow, P.W., Sole, A.J. orcid.org/0000-0001-5290-8967 et al. (2 more authors) (2024) Minimal impact of late-season melt events on Greenland Ice Sheet annual motion. *Geophysical Research Letters*, 51 (4). e2023GL106520. ISSN 0094-8276

<https://doi.org/10.1029/2023gl106520>

Reuse

This article is distributed under the terms of the Creative Commons Attribution (CC BY) licence. This licence allows you to distribute, remix, tweak, and build upon the work, even commercially, as long as you credit the authors for the original work. More information and the full terms of the licence here:

<https://creativecommons.org/licenses/>

Takedown

If you consider content in White Rose Research Online to be in breach of UK law, please notify us by emailing eprints@whiterose.ac.uk including the URL of the record and the reason for the withdrawal request.



eprints@whiterose.ac.uk
<https://eprints.whiterose.ac.uk/>

Geophysical Research Letters®

RESEARCH LETTER

10.1029/2023GL106520

Minimal Impact of Late-Season Melt Events on Greenland Ice Sheet Annual Motion



Key Points:

- September 2022 saw multiple melt events over the west Greenland Ice Sheet, with the largest daily runoff of any late melt-season since 1950
- Large quantities of surface-generated meltwater overwhelmed the subglacial drainage system causing brief increases in ice velocity
- Late-season runoff-induced speed-ups have only minimal impact on the mass balance of the Greenland Ice Sheet via dynamical processes

Supporting Information:

Supporting Information may be found in the online version of this article.

Correspondence to:

R. N. Ing,
ryan.ing@ed.ac.uk

Citation:

Ing, R. N., Nienow, P. W., Sole, A. J., Tedstone, A. J., & Mankoff, K. D. (2024). Minimal impact of late-season melt events on Greenland Ice Sheet annual motion. *Geophysical Research Letters*, *51*, e2023GL106520. <https://doi.org/10.1029/2023GL106520>

Received 24 NOV 2023

Accepted 31 JAN 2024

Author Contributions:

Conceptualization: Ryan N. Ing, Peter W. Nienow, Andrew J. Sole

Formal analysis: Ryan N. Ing, Peter W. Nienow

Investigation: Ryan N. Ing, Peter W. Nienow





Methodology: Ryan N. Ing, Andrew J. Sole, Andrew J. Tedstone

Resources: Andrew J. Tedstone, Kenneth D. Mankoff

Supervision: Ryan N. Ing, Peter W. Nienow, Andrew J. Sole

Visualization: Ryan N. Ing

Writing – original draft: Ryan N. Ing, Peter W. Nienow, Andrew J. Sole

Ryan N. Ing¹ , Peter W. Nienow¹, Andrew J. Sole² , Andrew J. Tedstone³ , and Kenneth D. Mankoff^{4,5} 

¹School of Geosciences, University of Edinburgh, Edinburgh, UK, ²Department of Geography, University of Sheffield, Sheffield, UK, ³Department of Geosciences, University of Fribourg, Fribourg, Switzerland, ⁴NASA Goddard Institute for Space Studies, New York, NY, USA, ⁵Autonomic Integra LLC, New York, NY, USA

Abstract Extreme melt and rainfall events can induce temporary acceleration of Greenland Ice Sheet motion, leading to increased advection of ice to lower elevations where melt rates are higher. In a warmer climate, these events are likely to become more frequent. In September 2022, seasonally unprecedented air temperatures caused multiple melt events over the Greenland Ice Sheet, generating the highest melt rates of the year. The scale and timing of the largest event overwhelmed the subglacial drainage system, enhancing basal sliding and increasing ice velocities by up to ~240% relative to pre-event velocities. However, ice motion returned rapidly to pre-event levels, and the speed-ups caused a regional increase in annual ice discharge of only ~2% compared to when the effects of the speed-ups were excluded. Therefore, although late melt-season events are forecast to become more frequent and drive significant runoff, their impact on net mass loss via ice discharge is minimal.

Plain Language Summary Extreme melt and rainfall events can cause the flow of ice on the Greenland Ice Sheet to accelerate, potentially causing more ice to move to lower elevations, where temperatures are warmer and melt rates are higher. In September 2022, there were multiple unprecedented melt events. Their intensity caused some glaciers on the ice sheet to speed up by 240% relative to pre-event speeds. Despite these accelerations, our analyses show that these events had only a minimal long-term impact on how much ice was moved to lower elevations due to the short duration of the speed-ups. As a result, while these melt-induced speed-ups are expected to become more common in a warmer climate, their effect on the amount of ice transported toward the ice margins is minimal.

1. Introduction

Across glacier systems worldwide, rapid influxes of surface runoff accessing the ice-bed interface can cause temporary increases in ice motion (Bingham et al., 2008; Gudmundsson et al., 2000). Numerous studies have drawn attention to the potential implications of such “speed-up” events for ice loss from the Greenland Ice Sheet (GrIS), as increased motion causes more ice to be advected to lower, warmer elevations, where surface melt rates are higher (e.g., Doyle et al., 2015; Zwally et al., 2002).

The seasonal cycles of surface melt and ice velocity on land-terminating sectors of the GrIS are coupled through the subglacial drainage system (Davison et al., 2019; van de Wal et al., 2015). Following the onset of the melt season, surface meltwaters begin to access the ice-bed interface (Nienow et al., 2017). Initially, the subglacial drainage system is spatially distributed and inefficient, and becomes overwhelmed by meltwater inputs which causes the basal water pressure to increase (Andrews et al., 2014; Bartholomew et al., 2011). This increase in pressure decreases basal friction leading to an acceleration in ice motion (Bartholomew et al., 2012; Schoof, 2010). As the melt season progresses, the rising supply of meltwater causes the formation of a more efficient channelized subglacial drainage system. The subsequent increased carrying capacity of these channels lowers the basal water pressure and decreases ice motion, with a minimum velocity typically occurring during the late melt-season (mid to late September in west Greenland) (Andrews et al., 2014; Stevens et al., 2016) before slowly accelerating over winter as the efficiency of the subglacial drainage system decreases (Joughin et al., 2008; Sole et al., 2013; Zwally et al., 2002). Although muted due to ocean and fjord processes influencing flow, a similar seasonal cycle in ice velocity can be seen at many marine-terminating glaciers (Moon et al., 2014).

© 2024. The Authors.

This is an open access article under the terms of the [Creative Commons Attribution License](https://creativecommons.org/licenses/by/4.0/), which permits use, distribution and reproduction in any medium, provided the original work is properly cited.

Writing – review & editing: Ryan N. Ing, Peter W. Nienow, Andrew J. Sole, Andrew J. Tedstone, Kenneth D. Mankoff

Within the seasonal cycle of ice motion described above, transient speed-up events occur at the margins of the GrIS when there is a large, short-term (<1 day) increase in the meltwater supply to the bed (Bartholomew et al., 2012; Doyle et al., 2015; van de Wal et al., 2008). These rapid influxes of water can result from sudden lake drainages, heavy rainfall, or melt events (e.g., Das et al., 2008; Doyle et al., 2015; Schmid et al., 2023; Shepherd et al., 2009; Tedstone et al., 2013) and overwhelm the capacity of the subglacial drainage system leading to increased basal lubrication (Bartholomew et al., 2008; Nienow et al., 2005; Sugiyama & Gudmundsson, 2004).

The ice speed-up from melt events can be larger in the late melt-season, when decreasing surface melt and ice creep cause the efficiency of the subglacial drainage system to decrease, making it susceptible to pressurization through minor variations in runoff (Fudge et al., 2009; Nanni et al., 2023). At this time of year, pulses of runoff are most frequently caused by rainfall and enhanced melt from atmospheric river events and cyclonic weather systems (Ballinger et al., 2019; Doyle et al., 2015) which are predicted to increase in frequency and intensity (Mattingly et al., 2018; Schuenemann & Cassano, 2010; Zhang et al., 2013). Therefore, associated transient speed-up events have been highlighted as a potential mechanism for increased mass loss over the coming decades (Bartholomew et al., 2008; Doyle et al., 2015; Schmid et al., 2023; Schoof, 2010). However, the significance of such events to the annual ice discharge of the GrIS remains unquantified.

In September 2022, the GrIS experienced multiple anomalous melt events, including the largest surface melt extent recorded during the late melt-season in the 45-year satellite observational record (Moon et al., 2022). These melt events provide an opportunity to investigate the impact of successive late-season melt events on ice dynamics; here of five land- and two marine-terminating outlet glaciers in west Greenland (Figure 1). These glaciers are characteristic of a large proportion of the margin of the GrIS, and experience summer melting which drives a seasonal cycle in ice velocity in response to variations in runoff (Davison et al., 2019; Shepherd et al., 2009). Additionally, the two marine-terminating glaciers exhibit contrasting grounding line depths and annual ice velocities, and are expected to display similar behavior to numerous other marine-terminating glaciers in the GrIS (Davison et al., 2020). Our study utilizes Sentinel-1 and GPS-derived ice velocities, in conjunction with meteorological conditions sourced from automatic weather stations and reanalysis models, to analyze the ice-dynamic response to these melt events. Furthermore, we employ Sentinel-1 derived ice velocities to estimate ice discharge using the flux-gate method to assess the impact of these late-season speed-ups on regional ice sheet mass loss through dynamical effects.

2. Methods

2.1. Ice Velocities

Ice velocities were derived from feature and speckle tracking of Sentinel 1a and 1b Interferometric Wide Swath mode Single-Look Complex Synthetic Aperture Radar amplitude images, following Davison et al. (2020). Only Sentinel 1a was used in 2022 due to the failure of Sentinel 1b in December 2021, resulting in overlapping velocity image pairs each with a 12-day temporal resolution (Text S1 in Supporting Information S1). Regions of Interest (ROI) of 2×2 km were placed in the central flowline of each glacier between 500 and 600 m above sea level (a.s.l.) and in regions with the best ice velocity data coverage. The median velocity of these grid cells was extracted to obtain a time series for each ROI.

The Sentinel-1 derived ice velocities were supplemented by higher temporal resolution velocity estimates calculated from the displacement of two GPS stations (KAN_L and Site 1, Figure 1) from May 2022 to May 2023. KAN_L is an automatic weather station located along the mid-flowline of Russell Glacier at an elevation of approximately 630 m a.s.l. (Fausto et al., 2021). Due to the low horizontal accuracy of the GPS receiver of 2.5 m, velocities were calculated by differencing hourly positions over a sliding 3-day window before averaging at a three-daily temporal resolution (Text S2 in Supporting Information S1). Site 1, located at 1449 m a.s.l., was used to investigate the ice dynamic response at higher elevations. These data were collected using a Leica Geosystems L1200 system at 10 s intervals, mounted on an aluminum pole frozen into the ice. We applied processing procedures as outlined previously in Tedstone et al. (2013) to yield daily (24-hr) along-track flow velocities (Text S3 in Supporting Information S1). A timeseries of Sentinel-1 and GPS-derived ice velocities were obtained using a LOWESS regression (Derkacheva et al., 2020).

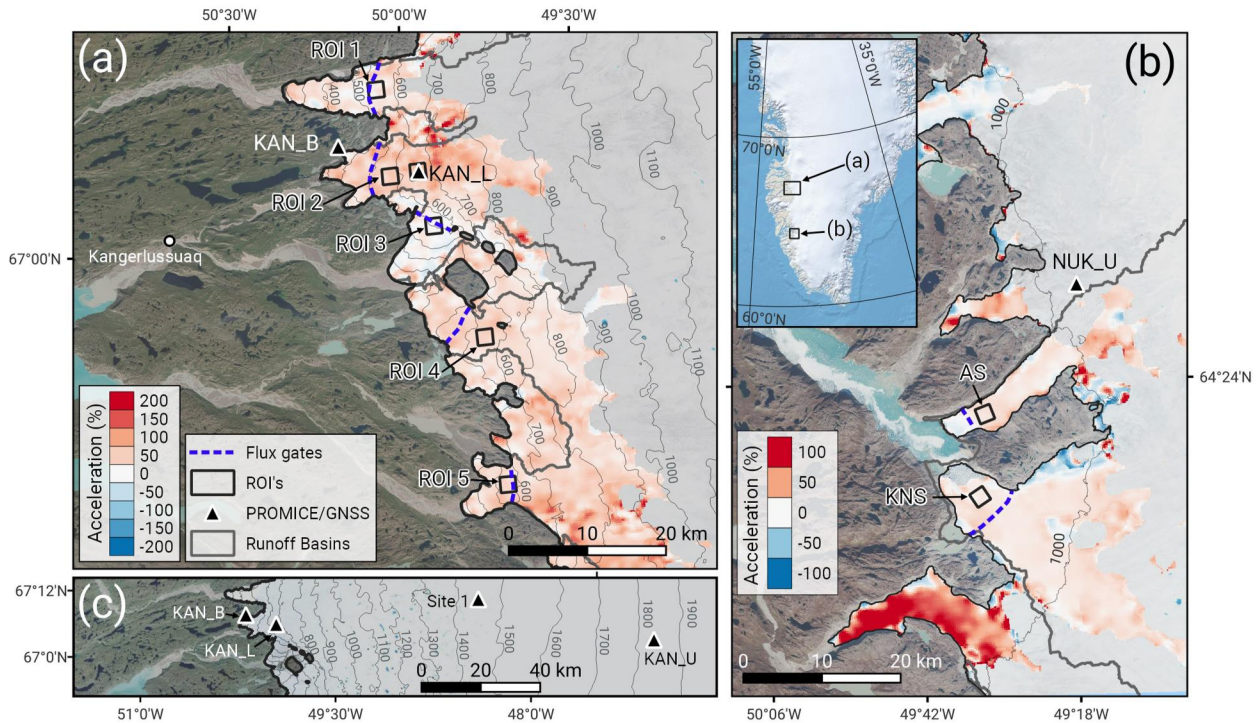


Figure 1. Study area of (a) land-terminating and (b) marine-terminating outlet glaciers (Kangiata Nunaata Sermia (KNS) and Akullursuup Sermia (AS)) draining the west GrIS. (c) Locations of high elevation GPS station and PROMICE weather stations. The background image is a Sentinel-2 true-color image obtained on 13th August (a) and (c), and 19th September 2022 (b). Overlaid is the acceleration in ice velocity during the early September melt events (22nd August to 13th September) as a percentage of mean pre-event velocity (1st to 21st August 2022). Black surface elevation contours were derived from the Greenland Ice Mapping Project (GrIMP) digital elevation model (DEM) (Howat et al., 2014). Regions of Interest (ROIs) are shown with black boxes, and the locations of the flux-gates are indicated by blue dotted lines. Black triangles indicate the locations of the PROMICE automatic weather stations used to measure meteorological variables and GPS station positions. The basins used for runoff estimates are outlined in gray.

2.2. Meteorological Data

The KAN_L and NUK_U PROMICE stations (Figure 1) were used to quantify the meteorological conditions driving the September melt events. Additionally, the COupled Snowpack and Ice surface energy and mass-balance model in PYthon (COSIPY) (Sauter et al., 2020) was forced with the weather station data and precipitation from the ERA5 Land reanalysis model to obtain hourly estimates of surface meltwater production and the surface energy balance (Text S4 in Supporting Information S1).

2.3. Ice Discharge

We estimated ice discharge at all seven outlet glaciers using the flux-gate method (King et al., 2018; Mankoff, Solgaard, et al., 2020; Mouginit et al., 2019). The flux-gates were placed between 500 and 600 m a.s.l. in regions with the best Sentinel-1 velocity data coverage (Figure 1). For each gate, the ice discharge (D) at each velocity image pair time step (t) was calculated using Equation 1.

$$D_t = \sum_{j=1}^n H_{j,t} V_{j,t} \omega_j \rho k \quad (1)$$

Where H is the ice thickness at each pixel bin (j), V is the surface velocity perpendicular to the gate, ω is the width of each pixel bin, ρ is the ice density (917 kg m^{-3}) and k is the reduction factor for surface velocity to represent the depth-averaged ice velocity (which was varied from 0.8 to 1, Van Wychen et al. (2014)). The calculated ice discharge at each gate for each image pair was then linearly resampled to daily temporal resolution (Text S6 in Supporting Information S1).

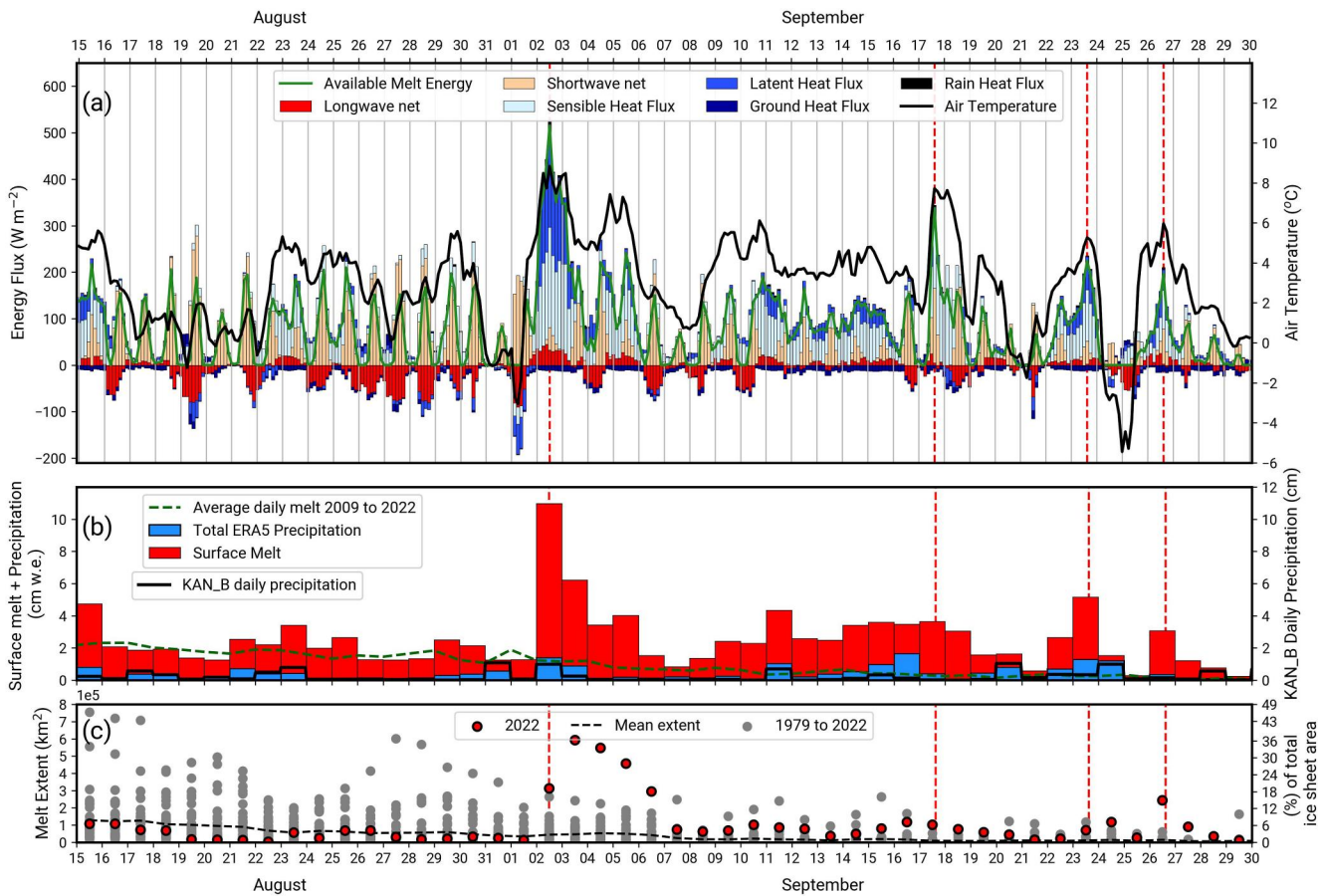


Figure 2. (a) Surface energy balance at KAN_L weather station (Figure 1a), with all variables resampled to 3-hourly means. (b) Modeled daily surface melt and ERA5 total precipitation at KAN_L, and total daily precipitation at on-land KAN_B (Figure 1a). (c) Daily melt extent of the GrIS derived from passive microwave sensors (Mote & Anderson, 1995). The red dashed vertical lines indicate the timing of each melt event.

3. Results

3.1. Surface Meltwater Production and Runoff

During September, the melt season across the west GrIS typically ceases (average daily surface melt <2 cm w.e. day⁻¹, Figure 2b) due to a decreasing solar zenith angle and air temperature (Figure 2b). However, in September 2022, daily surface melt rates were higher on six separate days than the average summer (June–August) maximum (3.7 cm w.e. day⁻¹, 2009–2022; Figure 3h). The first and largest of these events, starting on September 2nd, saw a rapid increase in air temperature from -3.9°C to 9.0°C in 24 hr (Figure 2a), the highest air temperature recorded that year. The event was spatially extensive, with a melt area covering $\sim 37\%$ of the ice sheet (Figure 2c, Mote and Anderson (1995)). At high elevations, KAN_U (1823 m a.s.l., Figure 1c) measured a temperature increase from -17.7°C to 2.7°C over the same 24-hr window. For the land-terminating catchment (Figure 1a), both the modeled daily runoff and the increase in daily runoff during the event were the largest observed in any late melt-season (defined as 16th August onwards) since 1950 (Mankoff, Noël, et al., 2020).

Like other extreme melt events (e.g., Ballinger et al., 2019; Fausto et al., 2016; Schmid et al., 2023), the event was driven by an atmospheric river (Figure S2 in Supporting Information S1) that advected warm, moist air over the ice sheet, increasing surface melt through increases in latent and sensible heat fluxes and downwelling longwave radiation (Figures 2a and 2b). The daily surface melt rate on September 2nd rose to 9.6 cm w.e. day⁻¹, greater than the previous 6 days combined and the highest daily melt in 2022 (Figures 2b and 3g). KAN_B, and ERA5 land reanalysis also displayed steady precipitation over the 24-hr period, contributing to the runoff (Figure 2b). Due to the late melt-season timing of the event, large areas of the ablation zone were bare ice, with minimal snowpack to buffer runoff (Figure S6 in Supporting Information S1). This enabled rapid delivery of meltwater to the bed,

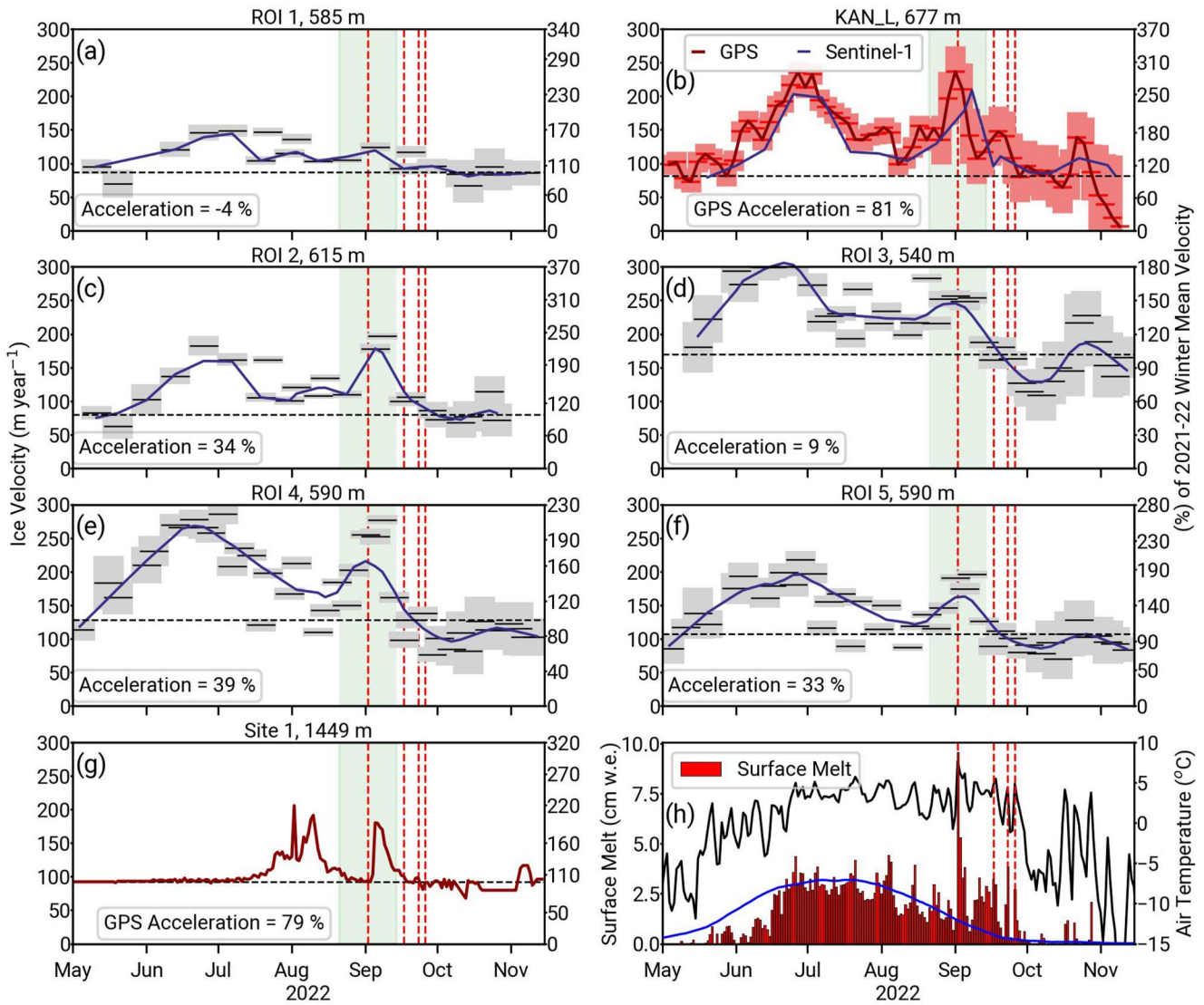


Figure 3. (a and c–f) Sentinel-1 derived ice velocity (black) for each ROI defined in Figure 1. The horizontal width of each line indicates the image pair timespan, with the error denoted by the vertical extent of the gray box. (b) 3-day averaged GPS derived velocities and estimated errors (red) from KAN_L. Overlaid is a velocity time-series calculated using a LOWESS regression (dark red) for KAN_L, (dark blue) for Sentinel-1. (g) 1-day averaged GPS derived velocity at Site 1. The text boxes in each subplot highlight the corresponding acceleration during the early September melt events (22nd August to 13th September) relative to the pre-event velocity. The median winter velocity (November to April) for 2021–22 is denoted by the black horizontal dotted line. The Sentinel-1 observational window for the September 2nd melt event is shown in green shading, with the onset of each melt event indicated by a red dotted vertical line. (h) Total modeled daily surface melt (red) and mean daily air temperature (black) for KAN_L and long-term average daily surface melt for KAN_L from 2009 to 2022 (blue).

following rapid transfer across the established supraglacial drainage network at this time of the season (as also observed by Doyle et al., 2015; Yang et al., 2021).

The remainder of September 2022 (3rd to 30th) saw multiple days of above-average surface melt, albeit of a smaller magnitude than that of the first event (Figure 2a). These events were centered around September 17th, 23rd and 26th, with the latter melt event driven by the remnants of ex-Hurricane Fiona bringing warm, moist air into the region (Pasch et al., 2023). An additional melt event was observed in late October when air temperatures briefly rose to 5°C with a surface melt rate of 1.3 cm w.e. day⁻¹ (Figure 3h).

3.2. Dynamic Response of Land-Terminating Glaciers

The first melt event induced a large increase in ice velocity across the land-terminating sector (Figure 3). At the five ROIs (Figure 1a), the mean acceleration in velocity was 22%, ranging from -4 to 40% (SD 17%) relative to

the preceding 1st to 21st August Sentinel-1 observational window prior to the first melt event (Figure 3). At all locations, ice velocity reached more than 140% of the mean value from the preceding winter, with a well-defined peak comparable to, and in some instances exceeding, the initial seasonal speed-up and typical period of maximum velocity in June/early July (Bartholomew et al., 2010; Hoffman et al., 2011) (Figure 3). The speed-up due to the event was spatially extensive extending up to the maximum coverage available for summer Sentinel-1 feature tracking at approximately 900 m a.s.l. (~15–20 km inland of the terminus) (Figure S3 in Supporting Information S1).

The higher temporal resolution (3-day averaged) KAN_L GPS (677 m a.s.l) derived velocities show a more pronounced response in ice velocity compared to the Sentinel-1 derived ice velocities (Figure 3b). For the September 2nd melt event, the ice accelerated by 81% to a velocity of 236 m yr⁻¹, faster than the earlier spring event peak (Figure 3b). At higher elevation (Site 1, 1449 m a.s.l), ice velocity accelerated by 79% to a velocity of 180 m yr⁻¹, lower than the earlier spring event peak (Figure 3g). This occurred approximately 3 days later than peak surface meltwater production, likely due to snow and firn delaying routing of meltwater to the bed. The lower-intensity melt events also induced a detectable response in the ice velocity at KAN_L and ROI 1 (Figure 3a).

After a period of 3 weeks with no modeled surface melt, the brief peaks in air temperature to above 5°C in mid-late October initiated an ice velocity response at all ROIs (Figure 3). The average acceleration was 37% for the Sentinel-1 derived velocities, and 61% for the KAN_L GPS derived speed compared to the preceding 1st–16th October mean.

3.3. Dynamic Response of Marine-Terminating Glaciers

Kangiata Nunaata Sermia (KNS) and Akullursuup Sermia (AS), marine-terminating glaciers located 300 km south of the land-terminating study region (Figure 1b) experienced similar atmospheric forcings, with three well defined September melt events (Figure S4c in Supporting Information S1). A clear dynamic response was observed at both glaciers, with an acceleration in ice velocity of 3% at KNS and 10% at AS compared to the pre-event mean ice velocity. A slight plateau in the declining ice velocity for KNS was centered around the later melt events in September (Figure S4b in Supporting Information S1).

3.4. Ice Discharge Estimates

Net annual ice discharge was calculated from May 2022 to May 2023; therefore, winter motion, which is impacted by the preceding melt season, was incorporated in the calculation. For the land-terminating sector, this provides insight into the amount of additional ice that was advected to lower, warmer elevations due to the September speed-ups. Similarly, for the marine-terminating glaciers, it provides quantification of the increase in ice discharge toward calving fronts.

The total ice discharge of the five ROIs in the land-terminating sector increased rapidly in response to the early September melt event (Figure 4), with peak ice discharge comparable in magnitude to the early melt season maximum (though of shorter duration) and is the largest observed discharge in September for the period 2016–2022. To estimate the impact of the September 2022 speed-ups on annual ice discharge, the September 2022 values were removed and replaced with linearly interpolated values from mid-August to October (covering the Sentinel-1 observational window of the September melt events). This estimation only accounts for the dynamic response in September and neglects any longer-term impacts on ice motion that may occur after large melt events, such as slower winter velocities (as observed in Sole et al., 2013; Tedstone et al., 2013; van de Wal et al., 2015). The September speed-ups led to an additional 0.017 Gt of ice being advected to lower elevations through our flux-gates which equates to an increase in the 2022 annual ice discharge across the sector of 1.70%, or just 1.64% of the long-term mean annual ice discharge (2016–2022). This is within the standard deviation of annual ice discharge for 2016–2022 of 0.027 Gt yr⁻¹ with a mean of 0.979 Gt yr⁻¹.

A minimal response to the September melt events was seen in ice discharge from the marine-terminating glaciers with an increase in annual ice discharge of just 0.32% or 0.03 Gt yr⁻¹ despite a mean acceleration in ice velocity of 6.41% (Figure S5 in Supporting Information S1).

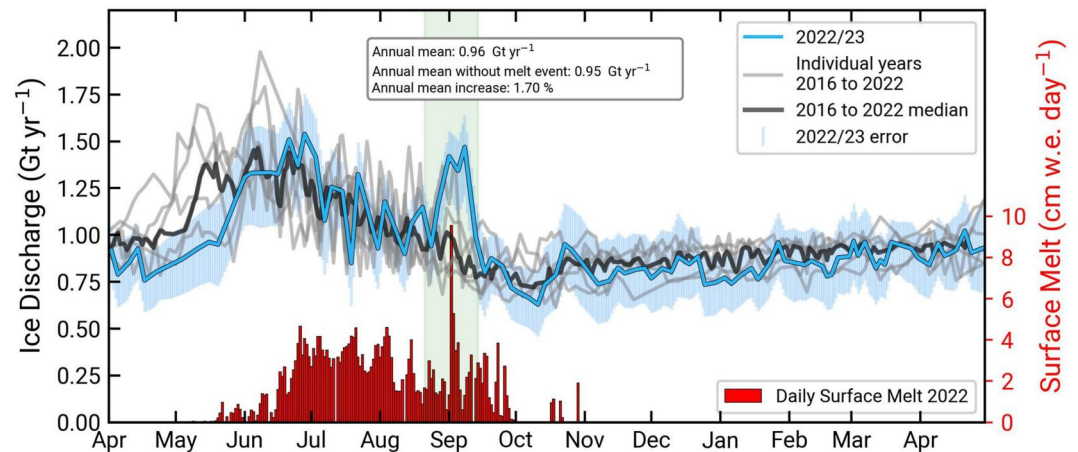


Figure 4. Total ice discharge of the land-terminating sector calculated using the flux-gate method. Light gray lines display the time-series of each individual year (2016–2022), solid gray line is the 2016 to 2022 mean discharge. The blue line represents the 2022/23 ice discharge with error bars (blue shading). The daily modeled surface melt at KAN_L for 2022 is indicated in red.

4. Discussion and Conclusions

With the predicted increase in poleward transport of moisture (Zhang et al., 2013) and observed increases in atmospheric river events (Mattingly et al., 2018), melt events and related speed-ups in ice velocity are likely to become more common (Doyle et al., 2015). During the peak of the melt season, efficient subglacial drainage limits the effect of these rapid runoff influxes on ice dynamics (Tedstone et al., 2013). Theoretically, during the late melt-season, such melt events could have a more substantial impact on ice dynamics (Doyle et al., 2015), with decreasing surface melt enabling the closure of subglacial channels through ice creep. For thinner ice (≈ 100 m) this transition is estimated to take weeks to days and for thicker ice (≈ 1 km), hours (Bartholomaeus et al., 2008; Bartholomew et al., 2012; Chandler et al., 2013; Hoffman et al., 2011). In September 2022, the week preceding the main event had low surface melt, averaging only 15% (1.5 cm w.e.) of the daily melt total (9.6 cm w.e.) at KAN_L on September 2nd (Figure 2b), which suggests minimal runoff was reaching the bed. Combined with the established supraglacial (Figure S6 in Supporting Information S1) and englacial drainage networks that allowed for the rapid routing of surface runoff to the bed, the melt event on September 2nd led to an acceleration in ice velocity of up to 240%. The subsequent melt and rainfall events induced smaller responses in ice velocity because of their lower magnitude, combined with the subglacial drainage system retaining some carrying capacity due to the sustained September melt (Figure 2b) (Schoof, 2010).

Although these speed-ups can be framed as substantial, they only last a few days (Figure 3) because the subglacial drainage system quickly adapts to accommodate the increased flux of water with the enlargement of pre-existing channels and subsequent depressurization of linked cavities (Bartholomaeus et al., 2008; Hoffman et al., 2016; Schoof, 2010). Therefore, their overall impact when viewed at annual timescales is limited with an increase in the net annual ice discharge of only 0.017 Gt or 1.70% (Figure 4) for the land-terminating glaciers and 0.027 Gt or 0.32% for the marine-terminating glaciers (Figure S5 in Supporting Information S1) compared to if the effects of the speed-ups were removed. At higher elevations (1449 m a.s.l.), a similar response was observed with the speed-ups causing an increase in net annual displacement of Site 1 GPS (Figure 1) of 1.89 m (1.89%). In contrast, the increase in the total annual runoff due to the September events was an order of magnitude higher, with liquid water discharge increasing by 24% (2.4 Gt) for the land-terminating glaciers, and 29% (1.4 Gt) for the marine-terminating glaciers for all ice-marginal outlets downstream of the flux-gates (Figure 1) (Text S5 in Supporting Information S1; Mankoff, Noël, et al., 2020).

A sequence of repeated large melt events, with minimal runoff between them, could in principle have a greater impact. However, this would require sufficient time with low surface runoff between events to allow the subglacial drainage system to become inefficient again through ice creep (Hoffman et al., 2011). It also requires no snowfall (to prevent the buffering of meltwater) and an established supraglacial drainage system to remain to ensure the rapid delivery of surface meltwater to the bed. Late melt-season runoff is primarily driven by rainfall

and melting through latent and sensible heat fluxes, which result from synoptic and general circulation weather patterns that have timescales of days to weeks (Hanna et al., 2018; McAvaney & Holland, 1995). It is therefore unlikely for multiple extreme melt events to occur in the late melt-season with minimal runoff and limited snowfall in-between. At higher elevations, the intervening low-runoff period *may* be less important, with thicker ice causing the subglacial channels to close more quickly (Doyle et al., 2014; Schoof, 2010). However, as observed in this study, the dynamic impact of the main melt event was similar at higher elevations (Figure 3g). Furthermore, as the late melt-season progresses, these melt events are less likely to impact higher elevations where the air temperatures are colder.

We conclude that multiple successive large melt events in September 2022 induced widespread acceleration in ice velocity of both the land and marine-terminating margins of the west GrIS. The speed-up was however transient, with the subglacial drainage system quickly reorganizing to accommodate the increased flux of meltwater. The net result on annual ice discharge was subsequently minimal for both land- and marine-terminating margins (1.70% and 0.32% increases respectively), as well as for a GPS station at higher elevations. These findings suggest that the expected increase in the frequency of such melt events is unlikely to cause large increases in annual ice motion. We note however that while the impact on ice dynamics was minimal, the effect on total annual runoff was substantial (24%–29% increase). Given that approximately 50% of the GrIS mass loss is attributed to surface meltwater runoff (Shepherd et al., 2020), the occurrence of such melt events, if ice-sheet wide, could substantially increase the annual ice-sheet mass loss, highlighting their importance for future surface mass imbalance (Beckmann & Winkelmann, 2023; Delhasse et al., 2018).

Data Availability Statement

The PROMICE weather station data sets are available from How et al. (2022), Greenland surface melt extent data from National Snow and Ice Data Center (2024), IceBridge BedMachine V5 bed topography and ice thickness data from Morlighem et al. (2022), surface elevation change from Yang et al. (2022), runoff estimates from Mankoff, Solgaard, et al. (2020) and ERA5 Land data from Muñoz-Sabater et al. (2021). The code and post-processed outputs used to create each figure are available on GitHub (Ing, 2024).

Acknowledgments

R.N.I is supported by a UK Natural Environmental Research Council PhD studentship (NE/T00939X/1). A.T was supported by the European Research Council award 818994—Cassandra, which also funded the collection of GPS data at Site 1 alongside the Swiss Polar Institute Exploratory Grant “HI-SLIDE.” K.D.M is supported by the NASA Modeling Analysis and Prediction program. DEMs provided by the Polar Geospatial Center under NSF-OPP awards 1043681, 1559691, and 1542736. We also thank the two anonymous reviewers for their constructive comments.

References

- Andrews, L. C., Catania, G. A., Hoffman, M. J., Gullely, J. D., Lüthi, M. P., Ryser, C., et al. (2014). Direct observations of evolving subglacial drainage beneath the Greenland Ice Sheet. *Nature*, *514*(7520), 80–83. <https://doi.org/10.1038/nature13796>
- Ballinger, T. J., Mote, T. L., Mattingly, K., Bliss, A. C., Hanna, E., van As, D., et al. (2019). Greenland Ice Sheet late-season melt: Investigating multiscale drivers of K-transect events. *The Cryosphere*, *13*(8), 2241–2257. <https://doi.org/10.5194/tc-13-2241-2019>
- Bartholomew, T. C., Anderson, R. S., & Anderson, S. P. (2008). Response of glacier basal motion to transient water storage. *Nature Geoscience*, *1*(1), 33–37. <https://doi.org/10.1038/ngeo.2007.52>
- Bartholomew, I., Nienow, P., Mair, D., Hubbard, A., King, M. A., & Sole, A. (2010). Seasonal evolution of subglacial drainage and acceleration in a Greenland outlet glacier. *Nature Geoscience*, *3*(6), 408–411. <https://doi.org/10.1038/ngeo863>
- Bartholomew, I., Nienow, P., Sole, A., Mair, D., Cowton, T., & King, M. A. (2012). Short-term variability in Greenland Ice Sheet motion forced by time-varying meltwater drainage: Implications for the relationship between subglacial drainage system behavior and ice velocity. *Journal of Geophysical Research*, *117*(F3). <https://doi.org/10.1029/2011JF002220>
- Bartholomew, I., Nienow, P., Sole, A., Mair, D., Cowton, T., Palmer, S., & Wadham, J. (2011). Supraglacial forcing of subglacial drainage in the ablation zone of the Greenland ice sheet. *Geophysical Research Letters*, *38*(8). <https://doi.org/10.1029/2011GL047063>
- Beckmann, J., & Winkelmann, R. (2023). Effects of extreme melt events on ice flow and sea level rise of the Greenland Ice Sheet. *The Cryosphere*, *17*(7), 3083–3099. <https://doi.org/10.5194/tc-17-3083-2023>
- Bingham, R. G., Hubbard, A. L., Nienow, P. W., & Sharp, M. J. (2008). An investigation into the mechanisms controlling seasonal speedup events at a High Arctic glacier. *Journal of Geophysical Research*, *113*(F2). <https://doi.org/10.1029/2007JF000832>
- Chandler, D. M., Wadham, J. L., Lis, G. P., Cowton, T., Sole, A., Bartholomew, I., et al. (2013). Evolution of the subglacial drainage system beneath the Greenland Ice Sheet revealed by tracers. *Nature Geoscience*, *6*(3), 195–198. <https://doi.org/10.1038/ngeo1737>
- Das, S. B., Joughin, I., Behn, M. D., Howat, I. M., King, M. A., Lizarralde, D., & Bhatia, M. P. (2008). Fracture propagation to the base of the Greenland Ice Sheet during supraglacial lake drainage. *Science*, *320*(5877), 778–781. <https://doi.org/10.1126/science.1153360>
- Davison, B. J., Sole, A. J., Cowton, T. R., Slater, D. A., Fahrner, D., & Nienow, P. W. (2020). Subglacial drainage evolution modulates seasonal ice flow variability of three tidewater glaciers in southwest Greenland. *Journal of Geophysical Research: Earth Surface*, *125*(9). <https://doi.org/10.1029/2019JF005492>
- Davison, B. J., Sole, A. J., Livingstone, S. J., Cowton, T. R., & Nienow, P. W. (2019). The influence of hydrology on the dynamics of land-terminating sectors of the Greenland Ice Sheet. *Frontiers in Earth Science*, *7*. <https://doi.org/10.3389/feart.2019.00010>
- Delhasse, A., Fettweis, X., Kittel, C., Amory, C., & Agosta, C. (2018). Brief communication: Impact of the recent atmospheric circulation change in summer on the future surface mass balance of the Greenland Ice Sheet. *The Cryosphere*, *12*(11), 3409–3418. <https://doi.org/10.5194/tc-12-3409-2018>
- Derkacheva, A., Mougnot, J., Millan, R., Maier, N., & Gillet-Chaulet, F. (2020). Data reduction using statistical and regression approaches for ice velocity derived by Landsat-8, Sentinel-1 and Sentinel-2. *Remote Sensing*, *12*(12), 1935. <https://doi.org/10.3390/rs12121935>

- Doyle, S. H., Hubbard, A., Fitzpatrick, A. A. W., van As, D., Mikkelsen, A. B., Pettersson, R., & Hubbard, B. (2014). Persistent flow acceleration within the interior of the Greenland ice sheet. *Geophysical Research Letters*, *41*(3), 899–905. <https://doi.org/10.1002/2013GL058933>
- Doyle, S. H., Hubbard, A., van de Wal, R. S. W., Box, J. E., van As, D., Scharer, K., et al. (2015). Amplified melt and flow of the Greenland ice sheet driven by late-summer cyclonic rainfall. *Nature Geoscience*, *8*(8), 647–653. <https://doi.org/10.1038/ngeo2482>
- Fausto, R. S., van As, D., Box, J. E., Colgan, W., Langen, P. L., & Mottram, R. H. (2016). The implication of nonradiative energy fluxes dominating Greenland ice sheet exceptional ablation area surface melt in 2012. *Geophysical Research Letters*, *43*(6), 2649–2658. <https://doi.org/10.1002/2016GL067720>
- Fausto, R. S., van As, D., Mankoff, K. D., Vandecrux, B., Citterio, M., Ahlström, A. P., et al. (2021). Programme for monitoring of the Greenland Ice Sheet (PROMICE) automatic weather station data. *Earth System Science Data*, *13*(8), 3819–3845. <https://doi.org/10.5194/essd-13-3819-2021>
- Fudge, T. J., Harper, J. T., Humphrey, N. F., & Pfeffer, W. T. (2009). Rapid glacier sliding, reverse ice motion and subglacial water pressure during an autumn rainstorm. *Annals of Glaciology*, *50*(52), 101–108. <https://doi.org/10.3189/172756409789624247>
- Gudmundsson, G. H., Bassi, A., Vonmoos, M., Bauder, A., Fischer, U. H., & Funk, M. (2000). High-resolution measurements of spatial and temporal variations in surface velocities of Unteraargletscher, Bernese Alps, Switzerland. *Annals of Glaciology*, *31*, 63–68. <https://doi.org/10.3189/172756400781820156>
- Hanna, E., Fettweis, X., & Hall, R. J. (2018). Brief communication: Recent changes in summer Greenland blocking captured by none of the CMIP5 models. *The Cryosphere*, *12*(10), 3287–3292. <https://doi.org/10.5194/tc-12-3287-2018>
- Hoffman, M. J., Andrews, L. C., Price, S. F., Catania, G. A., Neumann, T. A., Lüthi, M. P., et al. (2016). Greenland subglacial drainage evolution regulated by weakly connected regions of the bed | Nature Communications. *Nature Communications*, *7*(1), 13903. <https://doi.org/10.1038/ncomms13903>
- Hoffman, M. J., Catania, G. A., Neumann, T. A., Andrews, L. C., & Rumrill, J. A. (2011). Links between acceleration, melting, and supraglacial lake drainage of the western Greenland Ice Sheet. *Journal of Geophysical Research*, *116*(F4), F04035. <https://doi.org/10.1029/2010JF001934>
- How, P., Abermann, J., Ahlström, A. P., Andersen, S. B., Box, J. E., Citterio, M., et al. (2022). PROMICE and GC-Net automated weather station data in Greenland (Version 13) [Dataset]. GEUS Dataverse. <https://doi.org/10.22008/FK2/IW73UU>
- Howat, I. M., Negrete, A., & Smith, B. E. (2014). The Greenland ice mapping project (GIMP) land classification and surface elevation data sets. *The Cryosphere*, *8*(4), 1509–1518. <https://doi.org/10.5194/tc-8-1509-2014>
- Ing, R. N. (2024). Post-processed data and scripts - Minimal Impact of Late-Season Melt Events on Greenland Ice Sheet Annual Motion [Software]. Zenodo. <https://doi.org/10.5281/zenodo.10581317>
- Joughin, I., Das, S. B., King, M. A., Smith, B. E., Howat, I. M., & Moon, T. (2008). Seasonal speedup along the Western Flank of the Greenland Ice Sheet. *Science*, *320*(5877), 781–783. <https://doi.org/10.1126/science.1153288>
- King, M. D., Howat, I. M., Jeong, S., Noh, M. J., Wouters, B., Noël, B., & van den Broeke, M. R. (2018). Seasonal to decadal variability in ice discharge from the Greenland Ice Sheet. *The Cryosphere*, *12*(12), 3813–3825. <https://doi.org/10.5194/tc-12-3813-2018>
- Mankoff, K. D., Solgaard, A., Colgan, W., Ahlström, A. P., Khan, S. A., & Fausto, R. S. (2020). Greenland Ice Sheet solid ice discharge from 1986 through March 2020. *Earth System Science Data*, *12*(2), 1367–1383. <https://doi.org/10.5194/essd-12-1367-2020>
- Mankoff, K. D., Noël, B., Fettweis, X., Ahlström, A. P., Colgan, W., Kondo, K., et al. (2020). Greenland liquid water discharge from 1958 through 2019. *Earth System Science Data*, *12*(4), 2811–2841. <https://doi.org/10.5194/essd-12-2811-2020>
- Mattingly, K. S., Mote, T. L., & Fettweis, X. (2018). Atmospheric River impacts on Greenland Ice Sheet surface mass balance. *Journal of Geophysical Research: Atmospheres*, *123*(16), 8538–8560. <https://doi.org/10.1029/2018JD028714>
- McAvaney, B. J., & Holland, G. J. (1995). Chapter 8 - dynamics of future climates. In A. Henderson-Sellers (Ed.), *World survey of climatology* (Vol. 16, pp. 281–314). Elsevier. [https://doi.org/10.1016/S0168-6321\(06\)80031-3](https://doi.org/10.1016/S0168-6321(06)80031-3)
- Moon, T., Joughin, I., Smith, B., van den Broeke, M. R., van de Berg, W. J., Noël, B., & Usher, M. (2014). Distinct patterns of seasonal Greenland glacier velocity. *Geophysical Research Letters*, *41*(20), 7209–7216. <https://doi.org/10.1002/2014GL061836>
- Moon, T., Mankoff, K., Fausto, R., Fettweis, X., Loomis, B., Mote, T., et al. (2022). Arctic report card 2022: Greenland Ice Sheet NOAA Technical Report OAR ARC 22-05. <https://doi.org/10.25923/c430-hb50>
- Morlighem, M., Williams, C., Rignot, E., An, L., Arndt, J. E., Bamber, J., et al. (2022). IceBridge BedMachine Greenland, version 5 [Dataset]. NASA National Snow and Ice Data Center Distributed Active Archive Center. <https://doi.org/10.5067/GMEVBWFLWA7X>
- Mote, T. L., & Anderson, M. R. (1995). Variations in snowpack melt on the Greenland ice sheet based on passive-microwave measurements. *Journal of Glaciology*, *41*(137), 51–60. <https://doi.org/10.3189/S0022143000017755>
- Mouginot, J., Rignot, E., Björk, A. A., van den Broeke, M., Millan, R., Morlighem, M., et al. (2019). Forty-six years of Greenland Ice Sheet mass balance from 1972 to 2018. *Proceedings of the National Academy of Sciences of the United States of America*, *116*(19), 9239–9244. <https://doi.org/10.1073/pnas.1904242116>
- Muñoz-Sabater, J., Dutra, E., Agustí-Panareda, A., Albergel, C., Arduini, G., Balsamo, G., et al. (2021). ERA5-Land: A state-of-the-art global reanalysis dataset for land applications. *Earth System Science Data*, *13*(9), 4349–4383. <https://doi.org/10.5194/essd-13-4349-2021>
- Nanni, U., Scherler, D., Ayoub, F., Millan, R., Herman, F., & Avouac, J.-P. (2023). Climatic control on seasonal variations in mountain glacier surface velocity. *The Cryosphere*, *17*(4), 1567–1583. <https://doi.org/10.5194/tc-17-1567-2023>
- National Snow and Ice Data Center. (2024). Greenland today surface melt extent [Dataset]. National Snow and Ice Data Center, Boulder, Colorado. (Updated daily.) Retrieved from <https://nsidc.org/ice-sheets-today/melt-data-tools>
- Nienow, P. W., Hubbard, A. L., Hubbard, B. P., Chandler, D. M., Mair, D. W. F., Sharp, M. J., & Willis, I. C. (2005). Hydrological controls on diurnal ice flow variability in valley glaciers. *Journal of Geophysical Research*, *110*(F4). <https://doi.org/10.1029/2003JF000112>
- Nienow, P. W., Sole, A. J., Slater, D. A., & Cowton, T. R. (2017). Recent advances in our understanding of the role of meltwater in the Greenland Ice Sheet system. *Current Climate Change Reports*, *3*(4), 330–344. <https://doi.org/10.1007/s40641-017-0083-9>
- Pasch, R. J., Reinhart, B. J., & Alaka, L. (2023). *Tropical cyclone report: Hurricane Fiona*. NOAA National Hurricane Center. Retrieved from https://www.nhc.noaa.gov/data/tcr/AL072022_Fiona.pdf
- Sauter, T., Arndt, A., & Schneider, C. (2020). COSIPY v1.3—An open-source coupled snowpack and ice surface energy and mass balance model. *Geoscientific Model Development*, *13*(11), 5645–5662. <https://doi.org/10.5194/gmd-13-5645-2020>
- Schmid, T., Radić, V., Tedstone, A., Lea, J. M., Brough, S., & Hermann, M. (2023). Atmospheric drivers of melt-related ice speed-up events on the Russell Glacier in Southwest Greenland. *The Cryosphere Discussions*, 1–32. <https://doi.org/10.5194/tc-2023-1>
- Schoof, C. (2010). Ice-sheet acceleration driven by melt supply variability. *Nature*, *468*(7325), 803–806. <https://doi.org/10.1038/nature09618>
- Schuenemann, K. C., & Cassano, J. J. (2010). Changes in synoptic weather patterns and Greenland precipitation in the 20th and 21st centuries: 2. Analysis of 21st century atmospheric changes using self-organizing maps. *Journal of Geophysical Research*, *115*(D5). <https://doi.org/10.1029/2009JD011706>

- Shepherd, A., Hubbard, A., Nienow, P., King, M., McMillan, M., & Joughin, I. (2009). Greenland ice sheet motion coupled with daily melting in late summer. *Geophysical Research Letters*, *36*(1). <https://doi.org/10.1029/2008GL035758>
- Shepherd, A., Ivins, E., Rignot, E., Smith, B., van den Broeke, M., Velicogna, I., et al. (2020). Mass balance of the Greenland Ice Sheet from 1992 to 2018. *Nature*, *579*(7798), 233–239. <https://doi.org/10.1038/s41586-019-1855-2>
- Sole, A., Nienow, P., Bartholomew, I., Mair, D., Cowton, T., Tedstone, A., & King, M. A. (2013). Winter motion mediates dynamic response of the Greenland Ice Sheet to warmer summers. *Geophysical Research Letters*, *40*(15), 3940–3944. <https://doi.org/10.1002/grl.50764>
- Stevens, L. A., Behn, M. D., Das, S. B., Joughin, I., Noël, B. P. Y., van den Broeke, M. R., & Herring, T. (2016). Greenland Ice Sheet flow response to runoff variability. *Geophysical Research Letters*, *43*(21), 11295–11303. <https://doi.org/10.1002/2016GL070414>
- Sugiyama, S., & Gudmundsson, G. H. (2004). Short-term variations in glacier flow controlled by subglacial water pressure at Lauteraargletscher, Bernese Alps, Switzerland. *Journal of Glaciology*, *50*(170), 353–362. <https://doi.org/10.3189/172756504781829846>
- Tedstone, A. J., Nienow, P. W., Sole, A. J., Mair, D. W. F., Cowton, T. R., Bartholomew, I. D., & King, M. A. (2013). Greenland ice sheet motion insensitive to exceptional meltwater forcing. *Proceedings of the National Academy of Sciences of the United States of America*, *110*(49), 19719–19724. <https://doi.org/10.1073/pnas.1315843110>
- van de Wal, R. S. W., Boot, W., van den Broeke, M. R., Smeets, C. J. P. P., Reijmer, C. H., Donker, J. J. A., & Oerlemans, J. (2008). Large and rapid melt-induced velocity changes in the ablation zone of the Greenland Ice Sheet. *Science*, *321*(5885), 111–113. <https://doi.org/10.1126/science.1158540>
- van de Wal, R. S. W., Smeets, C. J. P. P., Boot, W., Stoffelen, M., van Kampen, R., Doyle, S. H., et al. (2015). Self-regulation of ice flow varies across the ablation area in southwest Greenland. *The Cryosphere*, *9*(2), 603–611. <https://doi.org/10.5194/tc-9-603-2015>
- Van Wychen, W., Burgess, D. O., Gray, L., Copland, L., Sharp, M., Dowdeswell, J. A., & Benham, T. J. (2014). Glacier velocities and dynamic ice discharge from the Queen Elizabeth Islands, Nunavut, Canada. *Geophysical Research Letters*, *41*(2), 484–490. <https://doi.org/10.1002/2013GL058558>
- Yang, B., Liang, S., Huang, H., & Li, X. (2022). An elevation change dataset in Greenland ice sheet from 2003 to 2020 using satellite altimetry data. *Big Earth Data*, *0*(0), 1–18. <https://doi.org/10.1080/20964471.2022.2116796>
- Yang, K., Smith, L. C., Cooper, M. G., Pitcher, L. H., As, D. van, Lu, Y., et al. (2021). Seasonal evolution of supraglacial lakes and rivers on the southwest Greenland Ice Sheet. *Journal of Glaciology*, *67*(264), 592–602. <https://doi.org/10.1017/jog.2021.10>
- Zhang, X., He, J., Zhang, J., Polyakov, I., Gerdes, R., Inoue, J., & Wu, P. (2013). Enhanced poleward moisture transport and amplified northern high-latitude wetting trend. *Nature Climate Change*, *3*(1), 47–51. <https://doi.org/10.1038/nclimate1631>
- Zwally, H. J., Abdalati, W., Herring, T., Larson, K., Saba, J., & Steffen, K. (2002). Surface melt-induced acceleration of Greenland ice-sheet flow. *Science*, *297*(5579), 218–222. <https://doi.org/10.1126/science.1072708>

References From the Supporting Information

- Adrian, R. J., & Westerweel, J. (2011). *Particle image velocimetry*. Cambridge University Press.
- Chen, G. (1998). GPS kinematic positioning for the airborne laser altimetry at Long Valley, California (Thesis). Massachusetts Institute of Technology. Retrieved from <https://dspace.mit.edu/handle/1721.1/9680>
- de Lange, R., Luckman, A., & Murray, T. (2007). Improvement of satellite radar feature tracking for ice velocity derivation by spatial frequency filtering. *IEEE Transactions on Geoscience and Remote Sensing*, *45*(7), 2309–2318. <https://doi.org/10.1109/tgrs.2007.896615>
- Fausto, R. S., Andersen, S. B., Ahlström, A. P., van As, D., Box, J. E., Binder, D., et al. (2018). The Greenland ice sheet—Snowline elevations at the end of the melt seasons from 2000 to 2017. *Geological Survey of Denmark and Greenland Bulletin*, *41*, 71–74. <https://doi.org/10.34194/geusb.v41.4346>
- Fehrenbach, J., Weiss, P., & Lorenzo, C. (2012). Variational algorithms to remove stationary noise: Applications to microscopy imaging. *IEEE Transactions on Image Processing*, *21*(10), 4420–4430. <https://doi.org/10.1109/tip.2012.2206037>
- Guizar-Sicairos, M., Thurman, S. T., & Fienu, J. R. (2008). Efficient subpixel image registration algorithms. *Optics Letters*, *33*(2), 156–158. <https://doi.org/10.1364/OL.33.000156>
- Howat, I. (2017). MEaSURES Greenland ice mapping project (GIMP) land ice and ocean classification mask, version 1 [Dataset]. NASA National Snow and Ice Data Center Distributed Active Archive Center. <https://doi.org/10.5067/B8X58MQBFUPA>
- Howat, I., Negrete, A., & Smith, B. (2022). MEaSURES Greenland ice mapping Project (GIMP) digital elevation model from GeoEye and WorldView imagery, version 2 [Dataset]. NASA National Snow and Ice Data Center Distributed Active Archive Center. <https://doi.org/10.5067/BHS4S5GAMFVY>
- Khvorostovsky, K., Hauglund, K., Forsberg, R., & Engdahl, M. (2018). Algorithm theoretical baseline document (ATBD) for the Greenland_Ice_Sheet_cci project of ESA's climate change initiative, version 3.2. Retrieved from <http://www.esa-icesheets-cci.org>
- Morlighem, M., Williams, C. N., Rignot, E., An, L., Arndt, J. E., Bamber, J. L., et al. (2017). BedMachine v3: Complete bed topography and ocean bathymetry mapping of Greenland from multibeam echo sounding combined with mass conservation. *Geophysical Research Letters*, *44*(21), 11051–11061. <https://doi.org/10.1002/2017GL074954>
- Porter, C., Morin, P., Howat, I., Noh, M., Bates, B., Peterman, K., et al. (2018). *ArcticDEM*. Harvard Dataverse, V3. <https://doi.org/10.7910/DVN/OHHUKH>
- Rosenau, R., Scheinert, M., & Dietrich, R. (2015). A processing system to monitor Greenland outlet glacier velocity variations at decadal and seasonal time scales utilizing the Landsat imagery. *Remote Sensing of Environment*, *169*, 1–19. <https://doi.org/10.1016/j.rse.2015.07.012>
- Sandwell, D., Mellors, R., Tong, X., Wei, M., & Wessel, P. (2011a). Open radar interferometry software for mapping surface deformation. *Eos Trans*, *92*(28), 234. <https://doi.org/10.1029/2011eo280002>
- Sandwell, D., Mellors, R., Tong, X., Wei, M., & Wessel, P. (2011b). *GMTSAR: An InSAR processing system based on generic mapping tools*. Scripps Institution of Oceanography Technical Report.
- Vandecrux, B., MacFerrin, M., Machguth, H., Colgan, W. T., van As, D., Heilig, A., et al. (2019). Firn data compilation reveals widespread decrease of firn air content in western Greenland. *The Cryosphere*, *13*(3), 845–859. <https://doi.org/10.5194/tc-13-845-2019>